AIP | The Journal of Chemical Physics

Neutral reactions in the presence of alkali ions

A. A. Viggiano, Carol A. Deakyne, F. Dale, and John F. Paulson

Citation: The Journal of Chemical Physics **87**, 6544 (1987); doi: 10.1063/1.453438
View online: http://dx.doi.org/10.1063/1.453438
View Table of Contents: http://scitation.aip.org/content/aip/journal/jcp/87/11?ver=pdfcov
Published by the AIP Publishing

Neutral reactions in the presence of alkali ions

A. A. Viggiano,[a] Carol A. Deakyne,[b] F. Dale, and John F. Paulson
AFGL/LID, Hanscom AFB, Massachusetts 01731-5000

(Received 30 April 1987; accepted 6 August 1987)

It has previously been shown that neutral ligands clustered to an alkali ion can react with other neutrals. In fact, the presence of the alkali ion greatly enhances the rate of the corresponding neutral–neutral reaction. Several more reactions that exhibit this phenomenon have been identified experimentally, with rate enhancements ranging from 4 to 30 orders of magnitude. Three possible explanations for the rate enhancement have been explored. *Ab initio* calculations have been carried out to supplement the experimental measurements and to provide further insight into the mechanism. The calculations indicate that bonding the neutral to the alkali ion causes structural rearrangements that shift the geometry of the neutral molecule toward its transition state geometry in the corresponding neutral–neutral reaction, thereby lowering the activation energy of the reaction.

INTRODUCTION

Alkali ions are isoelectronic with the noble gases and therefore are unreactive species. However, they form cluster bonds to a wide variety of neutrals. These cluster bonds have been shown to be mainly electrostatic in nature.[1] Rowe and co-workers[2] found that the ligands clustered to the alkali ions can react with other neutrals and that the presence of the alkali ion greatly enhances the rate of the corresponding neutral–neutral reaction. For example, the rate constants for reactions (1) and (2) differ by nine orders of magnitude.[2] Note, however, that the products of the reactions in the presence and absence of the alkali ion are not always identical:

$$N_2O_5 + NO \rightarrow 3NO_2, \tag{1}$$

$$Li^+ + N_2O_5 + NO \rightarrow Li^+(N_2O_4) + NO_2. \tag{2}$$

The rate enhancement for this reaction was found to depend strongly on the identity of the alkali ion to which the N_2O_5 is clustered. The rate constant for reaction (3) is also significantly enhanced in the presence of alkali ions[2]:

$$O_3 + NO \rightarrow NO_2 + O_2. \tag{3}$$

Rowe and co-workers[2] postulated three reasons for these large rate enhancements. The first is that the electrostatic interaction energy of the alkali ion–neutral complex and the reactant neutral is larger than the activation energy for the reaction between the neutral reactants in the absence of the ion. The second is that the potential energy surface is sufficiently altered in the presence of the ion to increase the rate constant significantly. Finally, the lifetime of the collision complex in the presence of the alkali ion is longer, yielding a greater reaction probability.

We have undertaken a study to determine the relative importance of the above causes of the rate enhancement. We have found several more reactions that exhibit this phenomenon, with rate enhancements of as much as 30 orders of magnitude. In addition, *ab initio* calculations have been carried out in order to supplement the rate constant measurements and to provide further insight into the mechanism.

EXPERIMENTAL AND THEORETICAL DETAILS

Experimental method

The experimental measurements were made in a fast flow system that could be operated with either a high pressure ion source or mass selected ion source (SIFT). The apparatus is shown in Fig. 1. The SIFT part of the instrument is essentially the previous instrument used in our laboratory.[3,4] The design of the high pressure source is similar to that of Fahey *et al.*[5] In the SIFT, ions are created in a moderate pressure (≈ 1 Torr) electron impact ion source. Upon exiting the ion source, the ions are focused into a quadrupole mass filter and are injected through a venturi inlet into a flow tube 1 m long. Introducing the ions through the venturi inlet aids the movement of ions from the low pressure quadrupole region to the high-pressure flow tube.[5] The ions are carried down the length of the flow tube by the buffer gas. The neutral reactant is added downstream. Reactant and product ions are sampled through a 0.2 mm hole in a blunt nose cone and detected by a second quadrupole and channel electron multiplier.

The high pressure source differs from the SIFT only in that the ions are created directly in the carrier gas. For these studies the ion source region was separated from the flow tube by a diaphragm with an orifice 5 mm in diameter. Under these conditions, the ion source region was maintained at a pressure of 10–20 Torr and the flow tube was operated at approximately 0.5 Torr.

The alkali ions were produced by thermionic emission from a rhenium filament coated with the appropriate alkali nitrate, silicon dioxide, and aluminum oxide. After a few hours of conditioning, the heated filament produced an essentially pure signal of the alkali ion of interest. The filament was electrically biased by a few volts with respect to the flow tube walls in order to generate a weak electric field and thus to help the ions enter the flow. Three filaments (Na, K, and Li) were put in the tube to enable us to change alkali ions

---

[a] Under contract to AFGL from Systems Integration Engineering Inc., Lexington, MA 02173.

[b] Air Force Geophysics Scholar.

0021-9606/87/236544-09$02.10

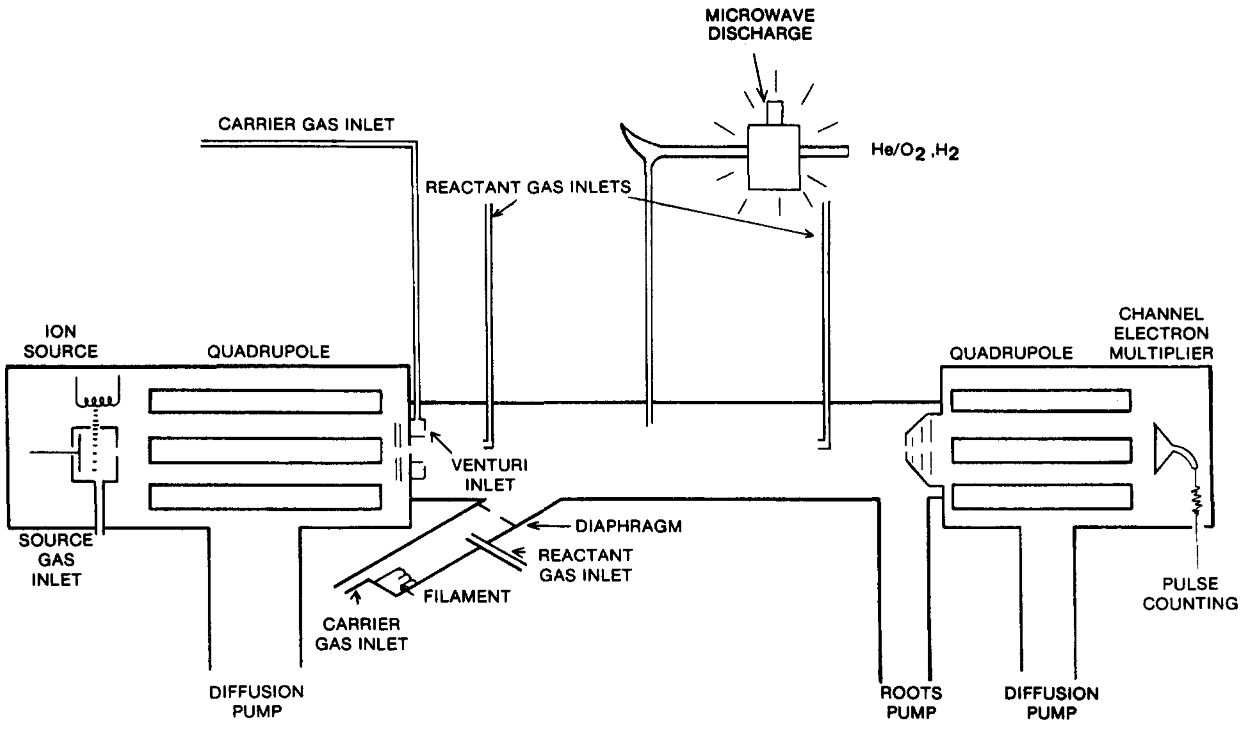

FIG. 1. Diagram of the newly constructed flowing afterglow-selected ion flow tube apparatus used in this work.

rapidly. The cluster ions were made by adding the clustering neutral to the ion source region slightly downstream of the filament. The clustering process occurred predominantly in the ion source region due to the higher pressure there compared with that in the flow tube. In this way, the desired reactant ions could be generated by adding much less of the clustering gas than would have been needed to yield the same amount of clustering in the absence of the diaphragm. In order to obtain the best signal for the cluster ion of interest without interference from other ions (i.e., larger cluster ions), the temperature, pressure, and buffer gas were varied. The three buffers used were He, N_2, and Ar.

The gases used in the experiments were standard commercial gases. The CO and NO were purified by passing them through an Ascarite filter to remove CO_2 and NO_2. Atomic oxygen was produced by passing a mixture of He and O_2 through a microwave discharge. The amount of O formed by dissociation of the O_2 was monitored by the reaction of CH_5^+ (generated in the SIFT) with O.[6] Typically the percent dissociation was in the 30%–40% range. This method is not so accurate as measuring the O atom concentration directly but is sufficient for the present purposes. Rate constants are believed to be accurate to within a factor of 2.

Theoretical method

The calculations were carried out *ab initio* on a VAX 11/780 computer. The GAUSSIAN 82 series of programs were utilized to perform the calculations.[7] The optimum structures of NO_2, $Li^+(CO_2)$, $Li^+(NO_2)$, $Li^+(NO)$, and LiO^+ were obtained at the HF/6-31G* basis set level[8] via the force relaxation method.[9] The equilibrium geometries of NO, NO_2, and CO_2 were taken from the literature.[10,11] All the additional calculations were carried out at the optimized 6-31G* geometries.

Electronic lithium ion affinities ΔE for reaction (4) were obtained with Eq. (5). Here, E_T is the total electronic energy and A is O, NO, NO_2, or CO_2:

$$Li^+ + A \rightarrow Li^+(A), \tag{4}$$

$$\Delta E = -[E_T(Li^+(A)) - E_T(Li^+) - E_T(A)]. \tag{5}$$

In order to compare the theoretical results to experimental gas-phase lithium ion affinities, the calculated electronic lithium ion affinities ΔE must be converted to calculated lithium ion affinities ΔH^{298} via Eq. (6)[12]:

$$\begin{aligned}\Delta H^{298} &= \Delta E - \Delta ZPE - \Delta(\Delta E_v)^{298} - \Delta E_t^{298} \\ &\quad - \Delta E_r^{298} - \Delta PV \\ &= \Delta E - \Delta ZPE - \Delta(\Delta E_v)^{298} \\ &\quad - \Delta E_r^{298} + 5/2RT.\end{aligned} \tag{6}$$

Here, ΔZPE is the change in the zero-point vibrational energies of the reactants and products. ΔE_t^{298} and ΔE_r^{298} are the energy changes due to the differences in the number of translational and rotational degrees of freedom, respectively. $\Delta(\Delta E_v)^{298}$ is the change in the difference in the vibrational energies of the reactants and products between 0 and 298 K. ΔPV is the change in the PV work term. Assuming ideal behavior, $\Delta PV = -RT$ for reaction (4). Classically, $\Delta E_t^{298} = -3/2RT$ and $\Delta E_r^{298} = -1/2RT$ for each rotational degree of freedom lost via production of the complex. For the reactions studied in this work, ΔE_r^{298} is 0 ($A = CO_2$, NO_2), $1/2RT$ ($A = NO$), or RT ($A = O$). The zero-point

TABLE I. Rates of ion enhanced reactions.

Reaction	Rate constant ($cm^3 s^{-1}$)	Temp (K)	Rate enhancement[c]	E_a ($kcal\ mol^{-1}$)
$Li^+(NO_2) + CO \rightarrow Li^+(CO_2) + NO$[a]	7(− 12)[b]	213–294	10^{30} [e]	28[e]
$Na^+(NO_2) + CO \rightarrow Na^+(CO_2) + NO$	1(− 12)	213–289	10^{29} [e]	28[e]
$Li^+(NO_2) + H_2 \rightarrow$ products	< 1(− 14)	219	···	18[e]
$Li^+(HBr) + O \rightarrow Li^+ + HBrO$ $\rightarrow Li^+ + Br + OH$	2(− 10)	178–219	10^5 [e]	3.1[e]
$Li^+(HBr)_2 + O \rightarrow Li^+HBrO + HBr$	2(− 10)	178	10^5 [e]	3.1[e]
$Na^+(HBr) + O \rightarrow Na^+ + HBrO$ $\rightarrow Na^+ + Br + OH$	1(− 10)	219	2×10^4 [e]	3.1[e]
$Li^+(H_2S) + O \rightarrow Li^+(HSO) + H$[a] $\rightarrow Li^+ + H_2SO$	2(− 10)	219	5×10^4 [e]	4.3[e]
$Li^+(H_2S)_2 + O \rightarrow Li^+(H_2SO) + H_2S$[a] $\rightarrow Li^+ + H_2SO + H_2S$	2(− 10)	219	5×10^4 [e]	4.3[e]
$Na^+(H_2S) + O \rightarrow Na^+(HSO) + H$[a] $\rightarrow Na^+ + H_2SO$	1(− 10)	178–219	1.5×10^5 [e]	4.3[e]
$Na^+(H_2S)_2 + O \rightarrow Na^+(H_2SO) + H_2S$[a] $\rightarrow Na^+ + H_2SO + H_2S$	2(− 10)	178	3×10^5 [e]	4.3[e]
$Li^+(N_2O) + O \rightarrow Li^+ + N_2 + O_2$	5(− 13)	219	10^{25} [e]	28[e]
$Li^+(N_2O_5) + NO \rightarrow Li^+(N_2O_4) + NO_2$	1.2(− 11)[d]	247–303	$>10^9$ [f]	22[f]
$Na^+(N_2O_5) + NO \rightarrow Na^+(N_2O_4) + NO_2$	3(− 13)[d]	303	$>4\times10^6$ [f]	22[f]
$K^+(N_2O_5) + NO \rightarrow K^+(N_2O_4) + NO_2$	<5(− 14)[d]	218	···	22[f]
$Li^+(O_3) + NO \rightarrow Li^+ + O_2 + NO_2$	6(− 11)[d]	220–280	2×10^4 [g]	2.9[g]
$Na^+(O_3) + NO \rightarrow Na^+ + O_2 + NO_2$	6.5(− 11)[d]	163–243	2×10^5 [g]	2.9[g]
$K^+(O_3) + NO \rightarrow K^+ + O_2 + NO_2$	4.5(− 12)[d]	125–163	2×10^5 [g]	2.9[g]

[a] For detailed information on the products, see the text.

[b] 7(− 12) means 7×10^{-12}.

[c] The rate constant in the presence of the alkali ion divided by the rate constant for the corresponding neutral reaction at the coldest temperature listed.

[d] Data from Rowe and co-workers.[2]

[e] Neutral rate constant calculated from the tabulation of Kerr and Moss (Ref. 27).

[f] A limit to the neutral reaction rate constant can be obtained from the thermal decomposition of N_2O_5 in the presence of NO. The data of Viggiano *et al.* (Ref. 25) are used here.

[g] Neutral rate constant from Birks *et al.* (Ref. 26).

vibrational energy changes and overall temperature effects for these reactions have been estimated based on the results of Del Bene and co-workers.[13,14]

The electronic lithium ion affinities ΔE were computed with the 6-31G* and 6-31 + G* basis sets.[15] The latter basis set is formed by augmenting the former basis set with a shell of diffuse *sp* orbitals. The addition of diffuse functions reduces the basis set superposition error (BSSE),[16] which is large for 6-31G* calculated electronic lithium ion affinities.[17] It also leads, in general, to obtaining the correct sign for the electron correlation contribution to the electronic lithium ion affinity.[17] The effect of electron correlation on the ΔE values was determined by means of Moller–Plesset perturbation theory to third (MP3) order.[18]

From her investigation of the lithium ion affinities of several oxygen and nitrogen bases, Del Bene[13] has shown that relative affinities at these levels of calculation are quite good. However, the ΔE values tend to be overestimated (particularly the 6-31G*ΔEs) compared to the values at higher levels of theory.

RESULTS AND DISCUSSION

Trends in the experimental rate enhancements

The results of this study, as well as those of Rowe and co-workers,[2] are listed in Table I. In addition to the reactions given in the table, Rowe and co-workers[2] studied two other reactions that showed no rate enhancement. None of the rate constants was found to vary significantly with temperature. Rate constants were measured by the disappearance of ionic reactant. The products of the reaction in the presence of the alkali ion are not necessarily identical to the products of the neutral–neutral reaction in the absence of the alkali ion (see below). The column in Table I headed rate enhancement refers to the ratio of the rate constant in the presence of the alkali ion to that of the corresponding neutral reaction at the coldest temperature studied. Since none of the rate constants reported in Table I has been found to vary with temperature and all of the neutral rate constants have positive activation energies, this definition represents the largest value of the rate enhancement for each reaction. The rate enhancement varies from four orders of magnitude to 30 orders of magnitude.

As a result of several different experimental difficulties we were unable to measure any of these reactions with K^+ as the alkali ion. In general, bond strengths of neutrals to alkali ions decrease as the molecular weight of the alkali ion increases, due to the increasing size of the alkali.[19] Therefore, one must decrease the temperature of the flow tube in order to get workable signals of the K^+ clusters. In the case of $K^+(NO_2)$ the NO_2 froze in the inlet line before we could obtain usable signals of $K^+(NO_2)$.

We could not do any experiments that involved K^+ and O due to the following unusual problem. Some unknown

TABLE II. Calculated total energies (E_T) in hartrees.

Molecule	Point group	Basis	HF	MP2	MP3
Li^+		6-31G*	− 7.235 54[a]		
		6-31 + G*	− 7.235 54[b]	− 7.235 54[b]	− 7.235 54[b]
O		6-31G*	− 74.783 93[a]		
		6-31 + G*	− 74.786 76	− 74.885 29	− 74.898 52
NO	$C_{\infty v}$	6-31G*	− 129.247 88		
		6-31 + G*	− 129.251 65	− 129.565 39	− 129.563 47
CO_2	$D_{\infty h}$	6-31G*	− 187.634 18[a]		
		6-31 + G*	− 187.638 79	− 188.112 16	− 188.098 32
NO_2	C_{2v}	6-31G*	− 204.031 49		
		6-31 + G*	− 204.038 33	− 204.565 57	− 204.544 33
LiO^+	$C_{\infty v}$	6-31G*	− 82.020 31		
		6-31 + G*	− 82.021 64	− 82.120 72	− 82.133 96
$Li^+(NO)$	C_s	6-31G*	− 136.504 79		
		6-31 + G*	− 136.506 78	− 136.814 82	− 136.815 00
$Li^+(NO_2)$[c]	C_s	6-31G*	− 211.300 64		
		6-31 + G*	− 211.304 87	− 211.827 29	− 211.809 32
$Li^+(CO_2)$	$C_{\infty v}$	6-31G*	− 194.905 16		
		6-31 + G*	− 194.907 99	− 195.378 55	− 195.366 35

[a] Reference 10.

[b] Reference 31.

[c] Structure II.

neutral KX emitted from the K filament reacted with O to form ion pairs:

$$KX + O \rightarrow K^+ + X(O)^-. \tag{7}$$

We could detect the formation of both K^+ and $X(O)^-$. Negative ion masses were observed at 79 ± 0 and 246 ± 2 amu in the ratio of 1 to 10. We have not been able to identify these ions although the ion at mass 79 has no major isotopes. One possibility (suggested by the referee) for mass 79 is $AlNO_3^-$. Reaction (7) has a rate constant of 2×10^{-10} $cm^3\ s^{-1}$ and unfortunately produces much more K^+ than is emitted directly from the filament. We had also hoped to study several reactions involving F_2, but neutrals emitted from all three alkali filaments created ion pairs upon addition of F_2. The reactions involving F_2 produced $Alk^+(AlkF)_{0,1,2}$, $F^-(AlkF)_{0,1}$, and larger mass negative ions in varying amounts. The rate constants for these reactions are also on the order of 2×10^{-10} $cm^3\ s^{-1}$. These reactions, although not understood, represent a significant fraction of the ground state chemiionization reactions known.[20,21]

Several trends in the data are readily observable. Neutrals clustered to Li^+ react either at the same rate or faster than those clustered to Na^+, which in turn react faster than those clustered to K^+ (Table I). The most dramatic example is the case of N_2O_5 reacting with NO, where the reaction in the presence of Li^+ is about 40 times faster than it is in the presence of Na^+. No detectable reaction was observed in the presence of K^+. The rate constant observed for the reaction of NO_2 with CO in the presence of Li^+ is a factor of 7 larger than it is in the presence of Na^+. For the O_3 reaction with NO the rates in the presence of Li^+ and Na^+ are the same, while the K^+ reaction is over an order of magnitude slower. All the reactions involving O atoms are fast (within a factor of 5 of the collision rate) with the exception of the reaction of N_2O with O.

In some cases, the two products both separate from the alkali as, for example, in the O_3 reaction with NO. This reaction is highly exothermic and provides sufficient energy to dissociate both neutrals; indeed, both do dissociate. The reaction of NO_2 with CO is also sufficiently exothermic to dissociate both ligands; however, in this case the CO_2 ligand stays attached to the alkali ion. In the reaction of N_2O_5 with NO, the reaction is exothermic only if one of the products remains attached to the alkali ion, and this is what is observed.

For several of the reactions it was also possible to determine what occurs when a second ligand is bonded to the alkali ion–neutral complex (Table I). The rate constant was found to be approximately the same whether one or two ligands were bonded to the alkali ion, although the products of the two reactions sometimes varied. For example, when H_2S reacts with O the main products are $Li^+(HSO)$ [or $Na^+(HSO)$] + H when one ligand is attached and $Li^+(H_2SO)$ [or $Na^+(H_2SO)$] + H_2S when two ligands are attached. The reaction involving two ligands may be thought of as an addition reaction in which the third body (the second H_2S) is built into the reactants.

Trends in the calculated electronic lithium ion affinities

Table II tabulates the total energies of Li^+, O, NO, NO_2, CO_2, LiO^+, $Li^+(NO)$, $Li^+(NO_2)$, and $Li^+(CO_2)$ at the various basis set levels. Table III gives the lithium ion affinities of O, NO, CO,[13] NO_2, and CO_2. LiO^+ is essentially not bound at any level of theory. The relative affinities of the other species are $CO_2 > NO_2 > CO > NO$.

The addition of diffuse functions to the basis set (6-31 + G* vs 6-31G*, Table III) decreases ΔE by about 1–1.5 kcal mol^{-1}. Taking electron correlation effects into account at the MP2 level also decreases ΔE by about 2-3.5 kcal mol^{-1}. In contrast, the third order Moller–Plesset calcula-

TABLE III. Computed values of ΔE in kcal mol^{-1} [a]

Complex	Basis	HF	MP2	MP3
LiO^+	6-31G*	0.53		
	6-31 + G*	-0.41[b]	-0.069[b]	-0.063[b]
$Li^+(NO)$	6-31G*	13.41		
	6-31 + G*	12.29	8.72	10.03
$Li^+(CO)$	6-311 + G(2*d*,2*p*)			14.5[c]
$Li^+(NO_2)$[d]	6-31G*	21.09		
	6-31 + G*	19.45	16.43	18.48
$Li^+(CO_2)$	6-31G*	22.24		
	6-31 + G*	21.12	19.36	20.39

[a] 6-31G* equilibrium structures were utilized at each calculational level.

[b] The negative sign indicates that LiO^+ is not bound at this level of calculation.

[c] Bonded through the carbon. This is the MP4SDQ/6-311 + G(2*d*,2*p*)//HF/6-31G*ΔE corrected for zero-point energy changes, temperature effects, and the PV work term (Ref. 13).

[d] Structure II.

tion increases the lithium ion affinity to a value in between the Hartree–Fock (HF) and MP2 values. These patterns are identical to those observed by other researchers.[13,17]

The MP3/6-31 + G* electronic lithium ion affinities obtained by Del Bene[13] are 1–1.5 kcal mol^{-1} larger than those obtained with the highest level of theory she considered, i.e., the MP4SDQ/6-311 + G(2*d*,2*p*) level. In addition, correcting for zero-point energy changes, temperature effects, and the PV work term [i.e., converting ΔE to ΔH^{298}, see Eq. (6)][12] lowers calculated ΔEs by 0.5–2.5 kcal mol^{-1}.[13,14] If the lithium ion affinities of the molecules studied in this work follow the same trends as those observed by Del Bene and co-workers,[13,14] then increasing the size of the basis set, taking the Moller–Plesset calculations to higher order, and correcting for zero-point energy changes, temperature effects, and the PV work term, will decrease the values reported in Table III by ~1–4 kcal mol^{-1}. Corrected lithium ion affinities computed with the MP4SDQ/6-311 + G(2*d*,2*p*) basis set are generally about 2 kcal mol^{-1} smaller than the experimental gas-phase values.[13,22]

Although changing the basis set does change the magnitudes of the ΔEs, the trends in the ΔEs vary very little with respect to basis set (Table III). The order of the electronic lithium ion affinities is the same at each basis set level, and the $\delta\Delta E$s are quite similar at each basis set level.

Reaction products vs buffer

One interesting observation not included in Table I is that the products of the NO_2 reaction with CO in the presence of Li^+ vary depending on which buffer is used. In a He buffer the major product ion (80%–90%) is $Li^+(CO)$; the minor product ion is $Li^+(CO_2)$. In a N_2 buffer only the $Li^+(CO_2)$ product is obtained. About equal amounts of the two products are formed in an Ar buffer.

The following explanation is consistent with the above observations, although we have no firm evidence that excludes other explanations. Reaction (8):

$$Li^+(NO_2) + CO \rightarrow Li^+(CO_2) + NO, \qquad (8)$$

is highly exothermic; ΔH^{298} is estimated to be -60 kcal mol^{-1} from the MP3/6-31 + G* data in Table II. (The MP3/6-31 + G* total electronic energy for CO is $-113.024\,22$ kcal mol^{-1}).[13] This suggests that the initial products contain a considerable amount of internal energy. Helium is not a very good quencher of vibrational energy in ions; therefore, one would expect the $Li^+(CO_2)$ product to remain vibrationally excited.[23] In contrast, one would expect that any vibrational excitation would be quenched in a N_2 buffer and that an Ar buffer would quench some but not all of the excitation.[23] The switching reaction

$$Li^+(CO_2) + CO \rightarrow Li^+(CO) + CO_2 \qquad (9)$$

is endothermic. ΔH^{298} is estimated to be 2–5 kcal mol^{-1} based on the data in Table III and the analysis given above for converting ΔE to ΔH^{298}. However, if the reactant ion has vibrational energy in excess of the endothermicity, the reaction may proceed. In light of the above discussion on quenching rates in different buffers, one would expect the amount of $Li^+(CO)$ formed to vary in the manner observed.

Reasons for the rate enhancement

One would like to obtain some understanding of the reasons for the rate enhancement. Only a detailed theoretical study can answer this interesting problem, but some simple qualitative arguments may shed some light on it. Three explanations have been postulated for why the reaction rate constants are significantly larger in the presence of the alkali ions.[2] The first is that the electrostatic interaction energy between the cluster ion and neutral is significantly larger than that for two neutrals. Second, the molecular potential energy surface is significantly altered by the presence of the ion. Finally, the lifetime of an ion–neutral collision complex is significantly longer than that for a neutral–neutral encounter. In reality these are not separable quantities, but it is of interest to look at the information we have on each one individually.

Interaction energy vs activation energy

The interaction energies between the ionic and neutral reactants are not known. Two simple methods are available to estimate the magnitudes of these energies. The first method is to take the interaction energy between a positive charge and a polarizable dipole at the radius of the alkali ion. Assuming purely electrostatic interactions this would overestimate the interaction energy, since the clustered alkali has a larger distance of closest approach than does the unclustered alkali. The other method is to use bond strengths of other ligand-alkali ion complexes to obtain some estimate of the bond strengths of the species in question. The first method[24] gives interaction energies of 45–129 kcal mol^{-1} for Li^+, 7–26 kcal mol^{-1} for Na^+ and 2–9 kcal mol^{-1} for K^+ with the neutrals used in this study. The lower number refers to O atoms and the higher to CO. Not much information has been reported on bond strengths of neutrals to alkali ions. From the data available, typical bond strengths of Li^+ to polar neutrals are on the order of 35 kcal mol^{-1}.[19] [Na^+ clusters have bond strengths between 12 (CO) and 24 (H_2O) kcal mol^{-1}.][19] K^+ bond strengths range from 8.5 (CO_2) to 17 (H_2O) kcal mol^{-1}.[19]

A first estimate of whether the neutral reaction can take place in the presence of the alkali ions is whether the above electrostatic interaction energies are larger than the neutral activation energies E_a. In fact, this was the method we used to determine which reactions might be catalyzed by the presence of the alkali ions. Previously[2] no such method was employed, and most of the reactions tried were not catalyzed.

The activation energy[25] for the reaction between N_2O_5 and NO is 22 kcal mol^{-1}. The estimated $Alk^+(N_2O_5)$–NO interaction energies are $\geqslant 35$ kcal mol^{-1} for Li^+, 15–25 kcal mol^{-1} for Na^+ and $\leqslant 10$ kcal mol^{-1} for K^+. These estimates are in line with the observed trends. Li^+ enhances the rate the most, and the Li^+ interaction energy is much larger than the activation energy. The rate constant in the presence of Na^+ is two orders of magnitude lower than it is in the presence of Li^+, and the interaction energy and activation energy are comparable for Na^+. The rate is not affected in any measurable manner when $K^+(N_2O_5)$ rather than N_2O_5 reacts with NO. In this case the interaction energy is significantly lower than the activation energy.

The rate constants for the reactions of $Na^+(O_3)$ and $Li^+(O_3)$ with NO are similar in magnitude (Table I), while that for the reaction of $K^+(O_3)$ with NO is an order of magnitude smaller. The activation energy[26] for the neutral reaction between O_3 and NO is 2.9 kcal mol^{-1}. The electrostatic interaction energies are significantly larger than E_a for Li^+ and Na^+. In contrast, E_a and the $K^+(O_3)$–NO interaction energy are similar (see analysis above). For the O reactions all of which, except for $N_2O + O$, are fast, the interaction energies are significantly greater than the activation energies of 3–4 kcal mol^{-1}.[27] The reaction of NO_2 with CO has the largest activation energy of any reaction for which we observed a rate enhancement. Here E_a is less than the $Alk^+(NO_2)$ interaction energy expected for Li^+ but is slightly larger than that expected for Na^+. We also looked for the reaction of $H_2O + CO$ which has an activation energy of 53 kcal mol^{-1} and saw no reaction in the presence of Li^+. Rowe and co-workers[2] also found no reactions to occur when they attempted to study several systems with large activation energies.

Reactant surfaces

In some of the aforementioned cases, a rate enhancement is observed even though the $Alk^+(A)$–B interaction energy is comparable to or slightly less than the activation energy for the neutral A–B reaction. This may best be explained by a change in the reactant surface when the neutrals are bound to an alkali ion (Fig. 2). The top drawing in Fig. 2 is a schematic representation of the reaction coordinate for the purely neutral reaction. Reactants A and B proceed over an activation barrier of magnitude E_a yielding reactants C and D. The simplest model for the reaction in the presence of an alkali ion is the two basin potential proposed by Brauman and co-workers[28] to explain many ion–molecule reactions (bottom drawing, Fig. 2). The reactants are neutral A clustered to an alkali ion $[Alk^+(A)]$ and B. As the reaction proceeds along the reaction coordinate, the reactants fall into an attractive well due to the electrostatic attraction between the cation cluster and neutral. After the first attractive well, $Alk^+(A)(B)$ encounters a barrier whose height can be either above or below the initial energy of the reactants. A second well follows, corresponding to the cluster $Alk^+(C)(D)$. Finally, one or both of the neutral products dissociates to form the alkali ion.

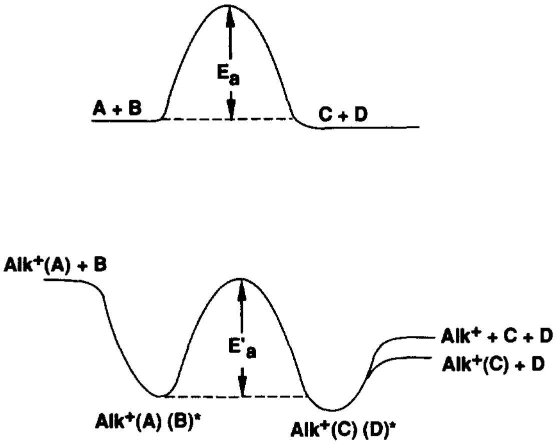

FIG. 2. The top drawing is a schematic of the reaction coordinate for a reaction between two neutrals A and B. The bottom drawing is a schematic of the reaction coordinate for a reaction between an alkali ion–neutral complex $[Alk^+(A)]$ and neutral B.

Based on the above schematic, the criterion for reaction is the height of the barrier between the two wells. If the barrier exceeds the initial energy of the reactants (case A), then the reaction would still have a positive activation energy and would not be measurable in our apparatus. The reaction could still be significantly faster in the presence of the ion but too slow for us to measure the difference in rates. If the barrier is considerably lower than the initial energy of the reactants (case B) the reaction should be rapid. As the barrier height changes from above to below the intitial energy of the reactants (case C), the rate constant should become increasingly large. In nucleophilic displacement reactions involving gas phase ions, the effect of the barrier becomes negligible only when it is approximately 5–10 kcal mol^{-1} below the zero of energy.[28]

How do the present data fit into this scheme? All the reactions in the presence of Li^+ would be represented by case B, i.e., the barrier has little or no effect since the well depth is substantial. The reactions in the presence of Na^+ for which the rate constant is comparable to that for the reaction in the presence of Li^+ are also type B reactions. Those for which the rate is substantially lower than the rate when a Li^+ complex is a reactant would be case C reactions. The barrier height has just begun to be important when the two rate constants vary by less than an order of magnitude. The reaction between O_3 and NO in the presence of K^+ falls into category B. The unobserved reactions of $K^+(N_2O_5)$ with NO and $Li^+(H_2O)$ with CO are case A reactions. As stated previously, experimental difficulties prevented us from studying any of the new reactions in the presence of K^+. This is unfortunate since it would have been a useful test of this scheme.

The temperature dependences of reactions in the three

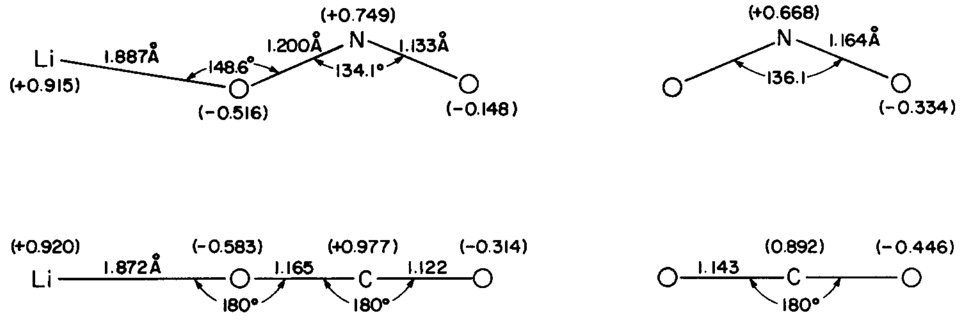

FIG. 3. 6-31G* equilibrium geometries of NO_2, CO_2, $Li^+(NO_2)$, and $Li^+(CO_2)$. The structures for CO_2 and NO_2 are from Ref. 10.

categories would be as follows. Case A reactions would have a large positive temperature dependence, case B reactions would show no temperature dependence, and case C reactions would have a negative temperature dependence. The magnitude of the negative temperature dependence would be fairly small ranging between approximately $T^{-l/2}$ (small molecules only) and T^0, where l is the total number of rotational degrees of freedom.[29] No dependence on temperature was seen for any of the reactions, although a small temperature dependence would have been missed due to the larger than normal uncertainty in the data. The observation that the rate constants did not depend on temperature is in qualitative agreement with the above picture.

E_a vs E'_a. Next we explore the interesting problem of the relative magnitudes of the barrier heights E_a and E'_a (Fig. 2). If a measurable rate constant is found, the top of the barrier in the bottom schematic of Fig. 2 cannot be significantly higher than the initial energy of the reactants. Furthermore, if the barrier is above the initial energy of the reactants, a large positive temperature dependence would be observed. Therefore, E'_a cannot be more than 1–2 kcal mol^{-1} greater than the electrostatic interaction energy of the $Alk^+(A)(B)$ complex. If the interaction energy is comparable to or less than the activation energy of the neutral–neutral reaction and a rate enhancement occurs, then E'_a must be less than or approximately equal to E_a.

Ab initio structures. In order to gain further information on the relative magnitudes of E_a and E'_a, consider the *ab initio* calculations on the structure and energetics of the complexes. The $Li^+(NO)$ structure was optimized in the C_s point group and remained bent with $\angle Li\cdots O\text{–}N = 175.2°$. The $Li^+\cdots O$ distance is 1.965 Å and the O–N distance is 1.137 Å. The latter distance can be compared with the bond length of 1.127 Å in neutral NO.[11] $Li^+(CO_2)$ was optimized in the C_s and C_{2v} point groups. The bent C_s structure is not a local minimum; it changes to the linear C_{2v} structure upon optimization.

Four possible conformations of $Li^+(NO_2)$ were examined and are shown in the diagram below. Their point groups are also given in the diagram. The most stable structure is II. The equilibrium geometries of CO_2,[10] NO_2, $Li^+(CO_2)$, and form II of $Li^+(NO_2)$ are presented in Fig. 3. Notice that there is a correlation between the electronic lithium ion affinities and the $Li\cdots O$ bond lengths. As the $Li^+\cdots O$ bond length decreases, ΔE increases (Table III and Fig. 3).

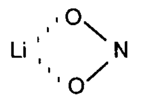

I, C_{2v}

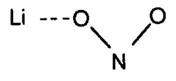

II, C_s

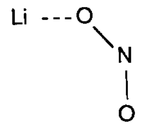

III, C_s

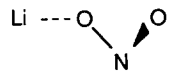

IV, C_1

Compare the structures of NO_2 and $Li^+(NO_2)$ in Fig. 3. In order to facilitate the reaction $NO_2 + CO \rightarrow CO_2 + NO$, it is desirable to lengthen (i.e., weaken) one of the NO bonds in NO_2 and to shorten the other. That is precisely what occurs in the presence of the Li^+ ion. In fact, the same type of structural rearrangement occurs in the $Li^+(CO_2)$ cluster (Fig. 3) and in other lithium clusters.[14,30,31] This suggests that forming the $Alk^+(A)$ complex enhances the reaction between A and B by shifting the structure of A toward what it is expected to be in the transition state for the neutral reaction. For the above reaction that is toward O + NO.

Bond strength vs bond distance. We are not presently able to estimate how much the activation energy is lowered due to the above bond lengthenings and shortenings, but we can estimate how much the N–O bond dissociation energy is reduced. Figure 4 is a plot of the logarithm of experimental bond strength[32] vs bond distance[33] for the N–O bonds in several molecules. The experimental bond lengths[33] in NO, NO_2, and NO_3 are plotted as circles, pluses, and squares, respectively. These values fall on a reasonably straight line which is used for calibration. The calculated values for the N–O distances in $Li^+(NO_2)$ and NO_2 are indicated by arrows. The estimated difference in the bond dissociation energy of the long N–O bond in $Li^+(NO_2)$ and the bond dissociation energy of NO_2 is then approximately 43 kcal mol^{-1}. The increase in bond strength for the other N–O bond in $Li^+(NO_2)$ is about the same. Therefore, the total bond strength of NO_2 is approximately constant in $Li^+(NO_2)$ and NO_2. Thus, the increase in bond length translates into ~ a 1/3 reduction in bond strength. This must surely translate into a lowering of the activation barrier as well, i.e., $E'_a < E_a$, and is one of the reasons for the rate enhancement.

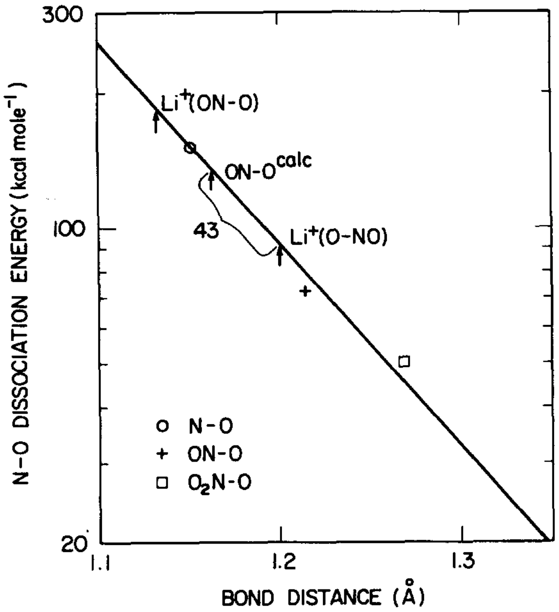

FIG. 4. N–O bond dissociation energies in kcal mol^{-1} vs N–O bond distances in Å. The experimental bond dissociation energies are from Ref. 32 and the experimental bond lengths are from Ref. 33.

Complex lifetime

The third postulated explanation for the observed rate enhancement is that the lifetime of the ion–neutral–neutral complex is longer than that of the neutral–neutral complex, yielding a larger reaction probability for the reaction in the presence of an alkali ion.[2(b)] Although a longer lifetime generally, but not always, leads to a greater reaction probability, the rate enhancements reported here far exceed what is expected solely from an increased lifetime.[34]

Components of the lithium cation affinities

The lithium cation affinity can be separated into four main attractive components—electrostatic, polarization, charge transfer, and dispersion.[35] For second row bases the electrostatic term is dominant; for third row bases both the electrostatic and polarization terms are important.[30] Since the maximum electrostatic interaction occurs along the dipole axis of a molecule,[36] most Li^+ complexes have the same molecular symmetry as the uncomplexed base.[13,14,30] This is what is observed for $Li^+(CO_2)$ (Fig. 3). However, neither $Li^+(NO)$ nor $Li^+(NO_2)$ have the Li^+ aligned along the symmetry axis of the base. The $\angle Li\cdots O{-}N$ in $Li^+(NO)$ is not 180°, although the deviation from linearity is small at ~ 5° (Fig. 3). The latter results suggest that polarization effects are more important in $Li^+(NO)$ and $Li^+(NO_2)$ than they are in other Li^+ complexes. In fact, the magnitudes of many of the parameters used to measure the size of the polarization contribution are larger for $Li^+(NO_2)$ than they are for $Li^+(CO_2)$. For example, forming the cluster changes the O–X ($X = N, C$) bond lengths more in $Li^+(NO_2)$ than in $Li^+(CO_2)$ (Fig. 3). Furthermore, the increase in electron density on the oxygen bonded to lithium and the decrease in electron density on the other oxygen are both greater for NO_2 (0.182 and 0.186 *e*, respectively) than they are for CO_2 (0.137 and 0.132 *e*, respectively, Fig. 3) when the complexes are formed. In contrast, the electrostatic contribution to the lithium cation affinity is larger for $Li^+(CO_2)$ than it is for $Li^+(NO_2)$. The $Li^+\cdots O$ distance is slightly smaller (Fig. 3), the 1*s* orbital energy of the Li^+ accepting oxygen $\epsilon_{1s}(O)$ is less stable ($-20.657\,82$ vs $-20.691\,38$ a.u.), and the charge on the oxygen in the isolated base is more negative (Fig. 3) for CO_2. The compromise between the two components accounts for the similar magnitudes of the electronic lithium cation affinities of the two bases.

CONCLUSIONS

We have studied several systems for which the presence of an alkali ion greatly enhances the neutral–neutral reaction rate. This can be an enormous effect, i.e., as large as 30 orders of magnitude. Li^+ is a more efficient rate enhancer than Na^+ which is more efficient than K^+. The main reason for the rate enhancement appears to be that the electrostatic interaction energy between the ion–neutral complex and the second neutral is larger than the activation energy of the reaction in the absence of the alkali ion. Calculations on the structures of the alkali ion–neutral complexes indicate that structural rearrangements are also important. For the reactions studied in this work, the rate enhancement does not seem to depend on the number of ligands attached to the alkali ion, although the products of the reactions do. In one of the reactions the observed products vary with buffer gas. This was explained by the fact that the reaction products are most likely vibrationally excited, and the different buffers quench this excitation to different extents. The primary reaction is followed by an endothermic ligand transfer that only proceeds when there is sufficient vibrational energy to overcome the endothermicity.

ACKNOWLEDGMENTS

The authors thank Dr. Michael J. Henchman for many helpful discussions and Mary Jean McCrossan for help in drawing the figures. The support of the Air Force Geophysics Laboratory Information Resources Center is gratefully acknowledged.

---

[1] K. G. Spears, J. Chem. Phys. **57**, 1842, 1850 (1972).

[2] (a) B. R. Rowe, A. A. Viggiano, F. C. Fehsenfeld, D. W. Fahey, and E. E. Ferguson, J. Chem. Phys. **76**, 742 (1982); (b) A. A. Viggiano, Thesis, Department of Chemistry, University of Colorado, 1980.

[3] A. A. Viggiano and J. F. Paulson, J. Chem. Phys. **79**, 2241 (1983).

[4] T. M. Miller, R. E. Wetterskog, and J. F. Paulson, J. Chem. Phys. **80**, 4922 (1984).

[5] D. W. Fahey, H. Böhringer, F. C. Fehsenfeld, and E. E. Ferguson, J. Chem. Phys. **76**, 1799 (1982).

[6] A. A. Viggiano, F. Howorka, D. L. Albritton, F. C. Fehsenfeld, N. G. Adams, and D. Smith, Astrophys. J. **236**, 492 (1980).

[7] GAUSSIAN 82, release H, J. S. Binkley, M. Frisch, R. Krishnan, D. J. DeFrees, H. B. Schlegel, R. A. Whiteside, E. M. Fluder, R. Seeger, and J. A. Pople, c. 1982, Carnegie–Mellon University.

[8] P. C. Hariharan and J. A. Pople, Mol. Phys. **27**, 209 (1974).

[9] (a) P. Pulay, Mol. Phys. **17**, 197 (1969); (b) H. B. Schlegel, S. Wolfe, and F. Bernardi, J. Chem. Phys. **63**, 3632 (1975).

[10] R. A. Whiteside, M. J. Frisch, and J. A. Pople, *Carnegie–Mellon Quantum Chemistry Archive*, 3rd ed. (Department of Chemistry, Carnegie–Mellon University, Pittsburgh, 1983).

[11] L. Farnell, J. A. Pople, and L. Radom, J. Phys. Chem. **87**, 79 (1983).

[12] J. E. Del Bene, H. D. Mettee, M. J. Frisch, B. T. Luke, and J. A. Pople, J. Phys. Chem. **87**, 3279 (1983).

[13] J. E. Del Bene, J. Comp. Chem. **7**, 259 (1986).

[14] J. E. Del Bene, M. J. Frisch, K. Raghavachari, J. A. Pople, and P. v. R. Schleyer, J. Phys. Chem. **87**, 73 (1983).

[15] G. W. Spitznagel, T. Clark, J. Chandrasekhar, and P. v. R. Schleyer, J. Comp. Chem. **3**, 363 (1983).

[16] S. F. Boys and F. Bernardi, Mol. Phys. **19**, 558 (1970).

[17] A. Latajka and S. Scheiner, Chem. Phys. Lett. **105**, 435 (1984).

[18] (a) C. Moller and M. S. Plesset, Phys. Rev. **46**, 618 (1934); (b) J. A. Pople, J. S. Binkley, and R. Seeger, Int. J. Quantum Chem. Symp. **10**, 1 (1976).

[19] R. G. Keesee and A. W. Castleman, Jr., J. Phys. Chem. Ref. Data **15**, 1011 (1986).

[20] *Gas-Phase Chemiluminescence and Chemi-Ionization*, edited by A. Fontijn (Elsevier Science, New York, 1985).

[21] U. Ross and Th. Schulze, J. Chem. Phys. **85**, 2664 (1986).

[22] R. L. Wooden and J. L. Beauchamp, J. Am. Chem. Soc. **100**, 501 (1978).

[23] E. E. Ferguson, in *Swarms of Electrons and Ions in Gases*, edited by W. Lindinger, T. D. Märk, and F. Howorka (Springer, Vienna, 1984).

[24] These are derived from ion–induced dipole and ion–locked dipole potentials. The polarizabilities and dipole moments are from C. G. Gray and K. E. Gubbins, *Theory of Molecular Fluids. Vol. 1. Fundamentals* (Clarendon, Oxford, 1984).

[25] A. A. Viggiano, J. A. Davidson, F. C. Fehsenfeld, and E. E. Ferguson, J. Chem. Phys. **74**, 6113 (1981).

[26] J. W. Birks, B. Shoemaker, T. J. Leck, and D. M. Hinton, J. Chem. Phys. **65**, 5181 (1976).

[27] *Handbook of Bimolecular and Termolecular Gas Reactions*, edited by J. A. Kerr and S. J. Moss (Chemical Rubber, Boca Raton, FL, 1981).

[28] A. T. Barfknecht, J. A. Dodd, K. E. Salomom, W. Tumas, and J. I. Brauman, Pure Appl. Chem. **56**, 1809 (1984), and references therein.

[29] The maximum temperature dependence is that of the complex lifetime. The temperature dependence of the complex lifetime can be estimated by the procedures given in: (a) D. R. Bates, J. Chem. Phys. **81**, 298 (1984); (b) E. Herbst, *ibid.* **82**, 4017 (1982); (c) A. A. Viggiano, *ibid.* **84**, 244 (1986), and references therein.

[30] S. F. Smith, J. Chandrasekhar, and W. L. Jorgensen, J. Am. Chem. Soc. **86**, 3308 (1982).

[31] E. Kaufmann, B. Tidor, and P. v. R. Schleyer, J. Comp. Chem. **7**, 334 (1986).

[32] S. W. Benson, *Thermochemical Kinetics: Methods for the Estimation of Thermochemical Data and Rate Parameters* (Wiley, New York, 1976).

[33] G. Herzberg, *Molecular Spectra and Molecular Structure. III. Electronic Spectra and Electronic Structure of Polyatomic Molecules* (Van Nostrand, New York, 1966).

[34] D. R. Bates, J. Chem. Phys. **81**, 298 (1984), and references therein.

[35] K. Morokuma, Acc. Chem. Res. **10**, 294 (1977).

[36] (a) P. J. Kollman, J. Am. Chem. Soc. **94**, 1837 (1972); (b) P. Kollman and S. Rothenberg, *ibid.* **99**, 1333 (1977).